IEEE Access
Multidisciplinary : Rapid Review : Open Access Journal

Received August 30, 2019, accepted October 2, 2019, date of publication October 9, 2019, date of current version October 28, 2019.

*Digital Object Identifier 10.1109/ACCESS.2019.2946502*

# Eccentricity Failure Detection of Brushless DC Motors From Sound Signals Based on Density of Maxima

**FRANK CESAR VERAS[1], THYAGO L. V. LIMA[2], JEFFERSON S. SOUZA[3], JORGE G. G. S. RAMOS[4], ABEL C. LIMA FILHO[5], AND ALISSON V. BRITO[3], (Member, IEEE)**

[1]Graduate Program of Mechanical Engineering, Universidade Federal da Paraiba (UFPB), Joao Pessoa 58051-900, Brazil
[2]Federal Institute of Paraiba (IFPB), Itabaiana 58360-000, Brazil
[3]Laboratory of System Engineering and Robotics, LASER, Universidade Federal da Paraiba (UFPB), Joao Pessoa 58051-900, Brazil
[4]Department of Physics, Universidade Federal da Paraiba (UFPB), Joao Pessoa 58051-900, Brazil
[5]Department of Mechanical Engineering (GPICEEMA), Universidade Federal da Paraiba (UFPB), Joao Pessoa 58051-900, Brazil

Corresponding author: Alisson V. Brito (alisson@ci.ufpb.br)

This work was supported in part by the Brazilian National Council for Scientific and Technological Development (CNPq) and in part by the Higher Education Improvement Coordination (CAPES).

**ABSTRACT** Brushless Direct Current (BLDC) motors have been used in a wide range of fields. In some critical applications, failures in these machines can cause operational disasters and cost lives if they are not detected in advance. The classical methods for detecting incipient faults in BLDC motors perform processing of the current signal to obtain the required information. In this work, the SAC-DM (Signal Analysis based on Chaos using Density of Maxima) technique is applied for the first time in the diagnosis of failures of electromechanical systems from sound signals. Wavelet Multiresolution Analysis (WMA) is used to separate a chaotic signal component from the sound emitted by the motor. This work demonstrates that it is feasible to perform dynamic eccentricity diagnosis in BLDC motors by identifying variations of the SAC-DM of the sound signal. The technique exposed in this work requires low computational cost and achieves high success rate. To validate the method, tests were carried out on a small BLDC motor normally used in Unmanned Aerial Vehicle (UAV), demonstrating the ability of the method to detect the speed of the motor in 95.89% of the cases and to detect eccentricity problems at a fixed speed in 88.34% of the cases.

**INDEX TERMS** Failure detection, sound, brushless motor, chaos.

## I. INTRODUCTION

Brushless Continuous Chain (BLDC) motors have excellent power-to-weight ratio and high reliability control [1], important features for electric vehicle traction system applications. Unexpected failures in these motors can be catastrophic, causing financial and human losses, for example when they occur in an industrial environment or in Unmanned Aerial Vehicles (UAVs). In the last years, researchers have dedicated efforts to improve BLDC efficiency and fault tolerance [2]–[4]. Also, there were advancements in UAV systems applications and commercialization [5], [6], in regulation on a global scale [7] and in discussions on the validation of critical security applications, to improve safety in autonomous control technology [8].

The associate editor coordinating the review of this manuscript and approving it for publication was Jenny Mahoney.

Basically, it is possible to classify fault identification methods in general by the sensor used or the signal processing technique. In the literature, it is possible to find works that aim to identify failures of dynamic eccentricity in several types of electric machines. The most common methods are those that perform acquisition of the electrical signals of the motor. From these, can be highlighted works, which processing are based on Fourier Transform [9], [10], Finite Elements [11], [12], Wavelet [13] and hybrid processing methods such as: Finite Elements/Fourier [14], Hilbert/Fourier [15], Wavelet/Fourier [16].

Methods using vibration signals are also found in the literature. In [17] the vibration signal is used for the diagnosis of dynamic eccentricity in an induction motor using Wavelet/Hilbert based algorithm. In [18] Fourier is used to process vibration signals and armature current also in an induction motor. In [19] vibration and sound signals with

Fourier-based processing are used to investigate the behavior of permanent magnet synchronous motors. In [20] the signals of sound, vibration and armature current of an induction motor are processed through Fourier-based algorithm, Hilbert-Huang transform and classifiers to identify several faults, including dynamic eccentricity.

In previous work, simulations were executed to demonstrate that the chaos present in the biodiversity of nature is associated with the chaotic evolution of the species and infer the correlation length from the density of maxima [21]. In [22] it was demonstrated that the same behavior detected from the current signal of Brushless Direct Current (BLDC) motors using FFT can also be captured from the chaotic behavior of the signal and in [23] a signal processing technique called SAC-DM (Signal Analysis based on Chaos using Density of Maxima) is presented. The work also demonstrated that SAC-DM can be applied to identify the speed at which the BLDC is operating and to detect the presence of unbalanced propeller analyzing the motor current signal.

In this work, the sound emitted by the motor is used for diagnosis. In order to evaluate whether SAC-DM is feasible for this type of application, or not, it is necessary to prove that the sound signal generated from the system (BLDC motor with propeller) has chaotic characteristics. In addition, there is a challenge inherent the sound signal to faults detection, when compared to electrical signals. Dynamic eccentricity alters the air gap of the machine, which leads to change the magnetic flux, that directly reflects in the supply current signal of the motor, making its computational processing simpler. The sound emitted by an electric motor depends on its mechanical interaction with the environment, whose nature is more complex in relation to electrical signals. For this reason, in [23] the SAC-DM technique is applied directly without the need for pre-processing. In this work, a chaotic component present in the signal of the sound emitted by the motor is extracted using a Wavelet approach. From the detail generated from Wavelet Multiresolution Analysis (WMA), it is demonstrated that it is possible to apply SAC-DM to identify dynamic BLDC eccentricity for different speed scenarios.

It was possible to identify dynamic eccentricity fault signals in BLDC motors using the method proposed in this work for different speeds almost instantaneously (analyzes performed every 0.023 seconds, approximately), presenting advantage over the Methods of Selection of Amplitudes of Frequency (MSAF) [24], [25] and Shortened Methods of Frequency Selection (SMOFS) [26], [27], which require longer acquisition time and constant speed analysis over a certain period of time.

Due to its performance and simplicity, the presented technique has potential for applications where response time is a requirement or the computational resources are limited. In our case, we propose the application on monitoring BLDC motors in small UAVs for failure detection during the flights.

An advantage of using sound signals to diagnose faults is the total non-invasiveness of the method, without contact with the motor, unlike those that using mechanical vibration signals or electrical sensors, for example. On the other hand, the SAC-DM technique, which is based on signal peak counting, presents a lower computational effort than the techniques found in the state of the art for fault detection in mechanical systems.

It was not found in the literature, techniques that allow the detection of dynamic eccentricity fault in electric machines motors using the only the sound signal. This work contributes to the monitoring of mechanical systems by acoustic analysis, proving that the sound signal of the BLDC has a chaotic characteristic (making possible the use of the SAC-DM technique) and in the development for the first time an algorithm based on WMA and SAC-DM for dynamic eccentricity fault detection.

### A. SIGNAL ANALYSIS BASED ON CHAOS USING DENSITY OF MAXIMA (SAC-DM)

The cyclic equilibrium behavior is the central issue of the current work and is used to identify the chaotic behavior of sound signal generated by a BLDC motor, even for a single and short time sample.

There are some techniques for the identification of chaos [28]–[31], but in the current work we apply a technique presented in a previous work [21] based on the Hamming distance concept [32], and on the counting of the density of maxima [33] of the sound signal.

In the work of Bazeia *et al.* [21] a quantitative approach is presented, which relates the correlation length to the average density of maxima of a signal. It results in a single and simple experimental realization that counts the density of maxima associated with the chaotic evolution of the species in an artificial life simulation to infer its correlation length. A technique called Signal Analysis based on Chaos using Density of Maxima (SAC-DM) is presented in [22], [23]. These works demonstrate that the current signal from a BLDC motor is chaotic, and that the correlation length can be estimated from the density of maxima, and apply it to detect failures and estimate the speed of the BLDC motor from the current signal.

In this work, we present the possibility of estimating the correlation length of the sound signal emitted by a BLDC motor using SAC-DM. Using this technique, a small amount of data from a signal q(t) is enough to characterize the chaos in this type of motor. This signal oscillates in time to produce the local maximum in the interval $[t, t + \delta t]$, for sufficiently small $\delta t$, so one has $q_i'(t) > 0$ and $q'(t + \delta t) < 0$ where prime stands for the time derivative, such that, $-q''(t)\delta t > q'(t) > 0$.

The joint probability $P(q', q'')$ can be used to calculate the average Density of Maxima $\langle \rho_1 \rangle$ through the simple route: the probability to find a maximum in the interval $[t, t + \delta t]$ is proportional to the integral spanning the region, such that

$$\rho_1 \equiv \frac{1}{\delta t}\int_{-\infty}^{0} dq'' \int_{0}^{-q''\delta t} dq' P(q', q'') = \int_{-\infty}^{0} dq'' q'' P(0, q'') \tag{1}$$

Moreover,

The properties of $P(q', q'')$ can be obtained from the smallest momenta of $q'$ and $q''$, and the variances of $P(q', q'')$ are directly related to the correlation function (Equation 2). Moreover, The fact that the statistical properties of the mean number of peaks are invariant under time translations indicates that both $q'$ and $q''$ have to vanish average values. From Equation 2 we can then obtain several momenta (Equation 3).

$$C(\delta t) = \langle q(t+\delta t)q(t)\rangle. \tag{2}$$

$$q'^2 = -\frac{d^2C(\delta t)}{d(\delta t)^2}\bigg|_{\delta t=0}; \quad q''^2 = -\frac{d^4C(\delta t)}{d(\delta t)^4}\bigg|_{\delta t=0}. \tag{3}$$

The joint probability distribution for q(t) and its derivatives from the previous equations based on the principle of maximum entropy. After implementing the algebraic calculations, integration on q(t) leads to $P(q', q'')$ (Equation 4).

$$P(0, q'') = \frac{1}{2\pi}.\frac{1}{\sqrt{\langle q'^2\rangle\langle q'^2\rangle}}\exp\Big(-\frac{1}{2}\frac{q''^2}{\langle q''^2\rangle}\Big) \tag{4}$$

Equation 5 is applied to obtain the theoretical average density of maxima ($\langle\rho_1\rangle$) from the auto-correlation function C from non-periodic signals. The derivative second and forth are represented as $C^{II}$ and $C^{IV}$ of the Auto-correlation Function in zero, as defined in other previous works [21], [22]

$$\langle\rho_1\rangle = \frac{1}{2\pi}\sqrt{-\frac{C^{IV}(0)}{C^{II}(0)}} = \frac{1}{2\pi}\sqrt{\frac{\langle q''^2\rangle}{-\langle q'^2\rangle}} \tag{5}$$

For periodic and homogeneous time series is possible to apply the principle of maximum entropy to write the normalized correlation as a cosine function, by reducing the previous equation to Equation 6, where $\langle\tau\rangle$ is the Correlation Length and $\langle\rho_2\rangle$ is the Density of Maxima found experimentally.

The derivatives of Equation 5 are only the theoretical basis, as the auto-correlation signal function is periodical, we opted for the simplified Equation 6 to find the correlation length. This reduction is the basis of the technique named Signal Analysis based on Chaos using Density of Maxima (SAC-DM). The value obtained from SAC-DM can be used to estimate the characteristics of a system using only a short time series, in this work, the sound signal is studied.

$$SAC\_DM = \langle\tau\rangle = \frac{1}{6\langle\rho_2\rangle} \tag{6}$$

## II. METHODOLOGY

In order to have a clearer notion of the approach proposed in this work, Figure 1 is presented. First, the sound signal from a small BDLC motor with a propeller is acquired using an Arduino Board. Then, the Wavelet Multiresolution Analysis (WMA) is performed to filter the signal and obtain the chaotic behavior from detail **D8** in the next steps. Following, the value of SAC-DM is calculated for each subset of the filtered signal using Equation 6. Finally, the value of SAC-DM of each subset is analyzed in order to identify the speed of the motor and if the propeller is unbalanced. Each step is described in the following sections.

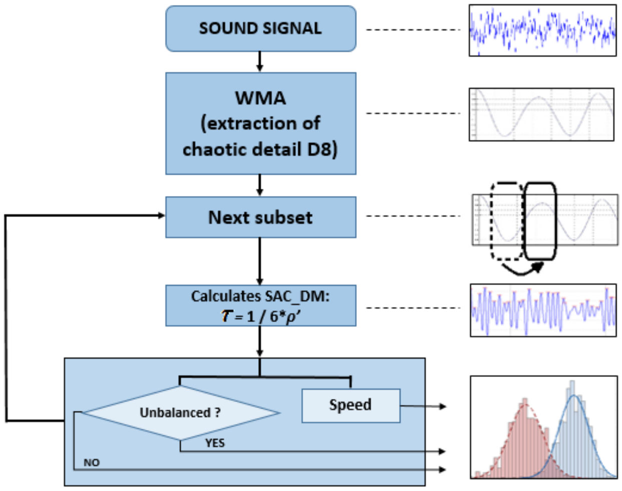


**FIGURE 1.** Methodology for signal analysis using density of maxima.

### A. SOUND SIGNAL ACQUISITION

In the experiments performed, a small electric BLDC motor with a propeller is used to test and analyze the acquired audios. The testbench used for the validation of the experiment is presented in Figure 2. The technical specifications of the BLDC motor are in Table 1. The sound signals are acquired from an electronic circuit with an Arduino board, integrated with a microphone that performs the audio recording.

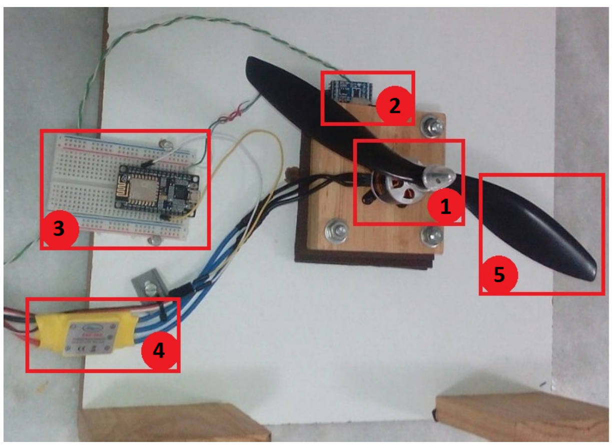


**FIGURE 2.** Testbench to acquire the sound of the system.

The testbench components of Figure 2 are: a (1) Brushless DC Motor 1400 Kv; an (2) Accelerometer Adafruit XL345; a (3) Node MCU ESP8266 12F (a micro-controller to set the speed sent to the ESC); an (4) Electronic Speed Controller (ESC) of 30 A; and a (5) 10.4 inch propeller. The power supply is Bi-volt with 115/230 VAc, 47-63 Hz and 4-6 A.

**TABLE 1. BLDC motor specifications.**

| Description | Value | Unit |
|---|---|---|
| DC Voltage | 12 | Volt |
| Rated Speed | 930 | RPM |
| Weight | 59 | Gram |
| Power | 270 | Watt |

Five experimental scenarios were executed, where three variables are combined: a) engine speed (60%, 65%, 70%, 75% and 80% of maximum power); b) propeller condition (regular or unbalanced); c) type of signal executed by the algorithm (raw or after the application of WDT). The regular propeller suggests perfect engine conditions. To generate the unbalanced condition, a 6 cm by 2.80 cm adhesive tape, approximate weight of 0.22838 grams, is fixed at 10 cm from the center of the propeller.

The embedded system used to acquired and process the sound signals is shown in Figure 3. It is composed by an Arduino Due development board and a CMA-4544PF-W electret condenser microphone.

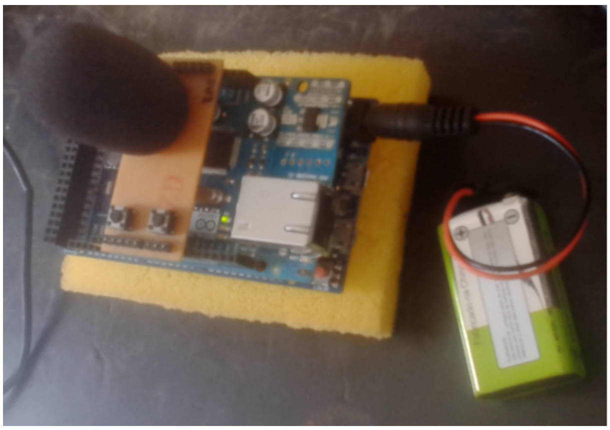

**FIGURE 3. Arduino platform with embedded microphone.**

The Arduino Due has a 32-bit ARM microcontroller: Atmel SAM3X8E ARM Cortex-M3. By the prior configuration of its registers and timers, the acquisition frequency was established in this work as 44.1 kHz. The CMA-4544PF-W is an omnidirectional electret condenser microphone with the sensitivity of 44 dB and operating frequency from 20 Hz to 20 kHz. Audio files are stored following the WAVE format, ensuring uncompressed audio storage in a memory card for later data analysis. Figure 4 shows a sound signal example without any filtering captured by the acquisition system at a speed of 80% of the motor power.

### B. APPLICATION OF WAVELET MULTIRESOLUTION ANALYSIS (WMA)

The Figure 5 represents the ACF found for the same signal from Figure 4 (motor at 80% speed). This function might tend to converge and dampen. However, the noise present in the signal, or the impurities in the measurement circuit, do not allow this damping as expected.

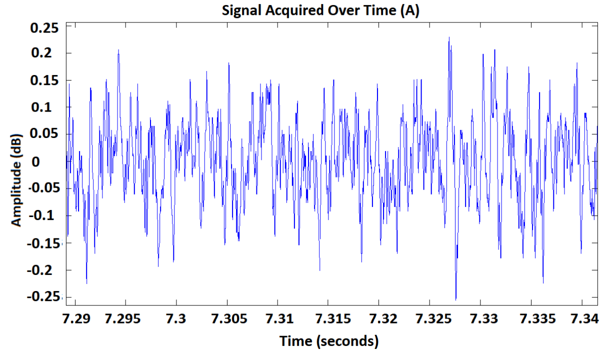


**FIGURE 4. Example of a sound signal captured at 80% of the maximum speed of the motor.**

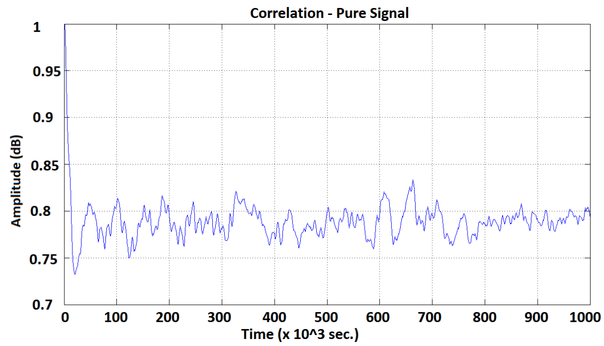


**FIGURE 5. Auto-correlation function for motor with balanced propeller at 80% speed.**

A powerful tool in the processing of stationary or dynamic signals is the Wavelet Multiresolution Analysis (WMA) [34], where the signal is subdivided into several levels of resolution. In this work, it was used because of its simultaneous effect in time and frequency. Based on the Mallat algorithm [35], at the first level of the WMA the sampled original signal

In this way, the Wavelet Multiresolution Analysis (WMA) [34] was applied to the sound signal, where the signal is subdivided into several levels of resolution. In this work, it was used the Mallat algorithm [35] at the first level of the WMA. Consequently, the signal decomposition at various levels of detail ($D_m[n]$) was performed, improving the conditions of analysis of the experiments and increasing the tendency of the function to converge and dampen.

Among the levels of signal decomposition by wavelet, the one that presented better convergence and damping was the Detail **D8**. In this case, this level of decomposition reached the most significant and adequate results for the desired parameters of this work, minimizing the external noise present in the sound samples.

The auto-correlation function of Detail **D8** from a sound signal at speed of 80% is shown in Figure 6. It is possible to observe that the application of the WDT resulted in the reduction of the noise, improving the

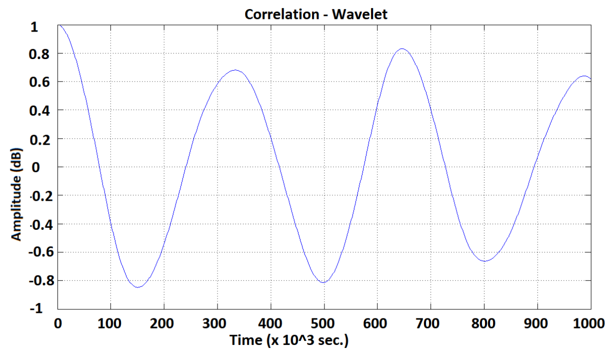


**FIGURE 6.** Auto-correlation after wavelet at 80% of speed - balanced propeller.

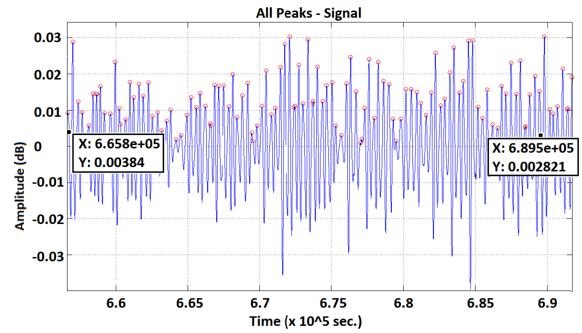


**FIGURE 8.** Sound signal in zoom with peaks with speed of 80% - balanced propeller.

convergence of the signal, with an amplitude greater than one in Figure 5.

### C. CALCULATING SAC-DM AND SYSTEM ANALYSIS

The SAC-DM is calculated for each subset of the filtered sound signal according to Equation 6, where $\rho$ is the number of peaks divided by the number of samples, i.e. the density of maxima. After calculation for each sub-set, it is checked whether the value of the SAC-DM is within the expected range for a balanced motor. If it is not, it returns that it is unbalanced. From the value of the SAC-DM, the estimated motor speed is also returned.

## III. PROVING THE CHAOTIC BEHAVIOR

Before presenting the experiments and results obtained with the application of the SAC-DM, this section presents tests that indicate the sound signal emitted by the BLDC motor actually has a chaotic behavior. This is true if the Correlation Length Coefficient (CLC) obtained from the Auto-correlation Function (ACF) results in a value similar to the one obtained by applying the density of maxima in the Equation 6.

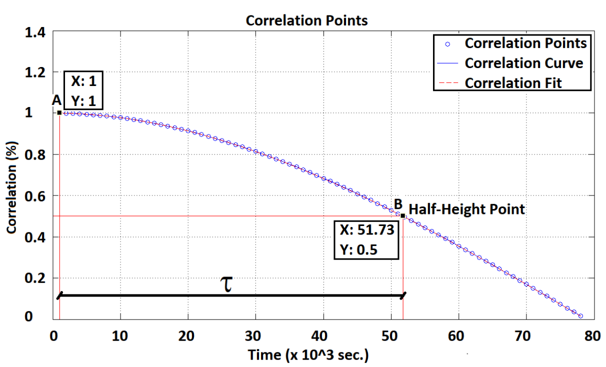


**FIGURE 7.** Correlation coefficient at half height after wavelet with speed of 80% - balanced propeller.

In Figure 7 is presented the CLC of the signal (from Figure 4) after the application of Wavelet, represented by $\tau$, which is the value at X when Y reaches the value of 0.5. In this example, the correlation length at half height obtained with a speed of 80% of the motor, and with the balanced propeller is 50.73 and expressed in Equation 7.

$$\tau = X_B - X_A = 51.73 - 1 = 50.73 \qquad (7)$$

Figure 8 presents a zoom in the same signal (Figure 4). It is possible to count 107 peaks and a total of 32,700 samples. Calculating the value of SAC-DM by Equation 6, we have:

$$\text{SAC\_DM} = \frac{1}{6\frac{107}{32,700}} = 50.9346 \qquad (8)$$

The relative percentage error found between the CLC shown in Figure 7 and the resulted from Equation 6 is 0.4033%. When the SAC-DM is calculated for the entire signal, the relative error decreases to 0.1011%.

Tables 2 and 3 present the results obtained from the sound signal in which the WDT is applied. They show the values for the CLC and SAC-DM followed by the relative percentage errors, for speed at 60%, 65%, 70%, 75% and 80%, and with two different propeller conditions: balanced or unbalanced.

**TABLE 2.** Comparison between CLC and SAC-DM after wavelet - balanced propeller.

| ESC Speed | CLC | SAC-DM | Relative Error |
|---|---|---|---|
| **60%** | 3.9339 | 3.9623 | 0.7197% |
| **65%** | 3.7775 | 3.7596 | 0.4740% |
| **70%** | 3.8387 | 3.8633 | 0.6397% |
| **75%** | 53.7995 | 53.9252 | 0.2336% |
| **80%** | 50.7259 | 50.7772 | 0.1011% |

**TABLE 3.** Comparison between CLC and SAC-DM after wavelet - unbalanced propeller.

| ESC Speed | CLC | SAC-DM | Relative Error |
|---|---|---|---|
| **60%** | 12.4089 | 12.4413 | 0.2610% |
| **65%** | 98.9916 | 98.2292 | 0.7702% |
| **70%** | 6.5368 | 6.5181 | 0.2857% |
| **75%** | 6.5575 | 6.5342 | 0.3552% |
| **80%** | 6.4220 | 6.4508 | 0.4479% |

It is observed that the Relative Error in Table 2 and Table 3 are less than 1%, and in most cases less than 0.5%, regardless of the condition of the propeller. It means the value obtained by SAC-DM is similar to the value of CLC obtained from ACF. Thus, it is demonstrated that the sound signal analyzed here has a chaotic behavior and, for this reason, it is possible to apply the SAC-DM to analyze the motor behavior now only using the Equation 6.

## IV. EXPERIMENTS AND RESULTS

In the experiments, for each speed (60%, 65%, 70%, 75%, and 80%), 60 seconds of audio were acquired. After application of Wavelet, each audio signal contained 1,764,000 samples. The SAC-DM was calculated for each subset of 1,000 samples. In the following sub-sections are presented the results SAC-DM for detection of speed and eccentricity problems.

### A. SPEED AND UNBALANCE DETECTION USING SAC-DM

Table 4 and Table 5 present the statistical analysis of the SAC-DM with the balanced and unbalanced propeller, respectively. The mean ($\mu$), variance ($\sigma^2$) and standard deviation ($\sigma_X$) are also presented for each analyzed speed. In Table 4 is observed that the SAC-DM has achieved significant results since the means of SAC-DM are different and increase with the motor speed. However, this does not happen with the unbalanced propeller (Table 5), which requires a more detailed investigation.

**TABLE 4.** Statistical analysis of SAC-DM results for regular BLDC motor.

| ESC Speed | $\mu$ | $\sigma^2$ | $\sigma_X$ |
|---|---|---|---|
| 60% | 0.9628 | $2.408 * 10^{-3}$ | 0.0491 |
| 65% | 1.0097 | $2.742 * 10^{-3}$ | 0.0524 |
| 70% | 1.1559 | $4.908 * 10^{-3}$ | 0.0701 |
| 75% | 1.2877 | $6.751 * 10^{-3}$ | 0.0822 |
| 80% | 1.4085 | $1.095 * 10^{-2}$ | 0.1046 |

**TABLE 5.** Statistical analysis of SAC-DM resulted for BLDC motor with unbalanced propeller.

| ESC Speed | $\mu$ | $\sigma^2$ | $\sigma_X$ |
|---|---|---|---|
| 60% | 1.0597 | $3.7 * 10^{-3}$ | 0.0609 |
| 65% | 1.2249 | $9.4 * 10^{-3}$ | 0.0969 |
| 70% | 1.1973 | $6.1 * 10^{-3}$ | 0.0784 |
| 75% | 1.3123 | $8.0 * 10^{-3}$ | 0.0894 |
| 80% | 1.1964 | $7.5 * 10^{-3}$ | 0.0864 |

Figure 9 and 10 present the values of the SAC-DM for each subset of the sound signal, for the balanced and unbalanced propeller, respectively. All results presented here were obtained analyzing the detail **D8** of WDT. From that, it is possible to confirm that when the propeller is unbalanced, there is more intersection of values along the time, in comparison with the balanced propeller.

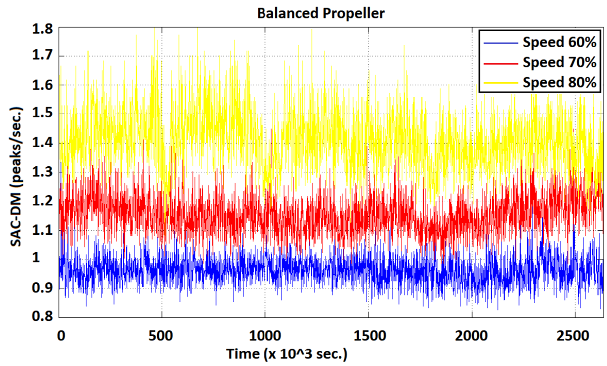


**FIGURE 9.** SAC-DM of detail **D8** (WDT) from the sound signal with normal propeller at 60%, 70% and 80% of maximum speed.

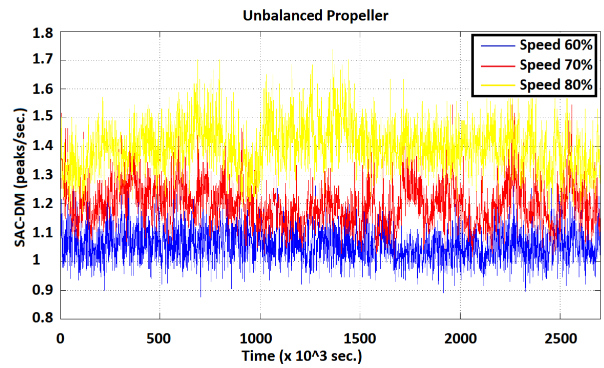


**FIGURE 10.** SAC-DM of detail **D8** (WDT) from the sound signal with unbalanced propeller at 60%, 70% and 80% of maximum speed.

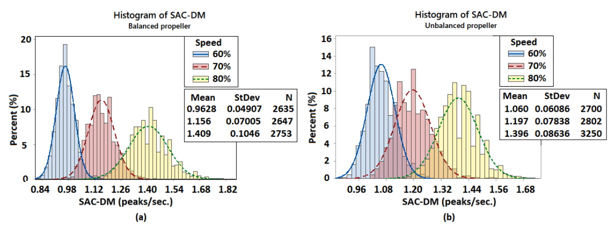


**FIGURE 11.** Histogram of SAC-DM obtained from the sound signal with: a) Balanced propeller for 60%, 70% and 80% of speed; b) Ubalanced propeller for 60%, 70% and 80% of speed.

In order to calculate this intersection, we produced the histograms of SAC-DM for each case. Figure 11 shows the SAC-DM histogram for the (a) balanced and (b) unbalanced propeller. In case a), the intersection between 60% and 70% of speed is 0.18%. Between 70% and 80% of speed, the area is 0.36%, this means that with SAC-DM is possible to determine the motor speed with 95,89% of accuracy when the propeller is balanced.

Likewise, the case b) presents the histogram of SAC-DM for the motor at 60%, 70% and 80% of speed, with an unbalanced propeller. In this case, the intersections between the areas are larger, which reduces the accuracy of speed estimation. Now, the intersection between 60% and 70% of speed is of 0.84%. Between 70% and 80% of speed, the area

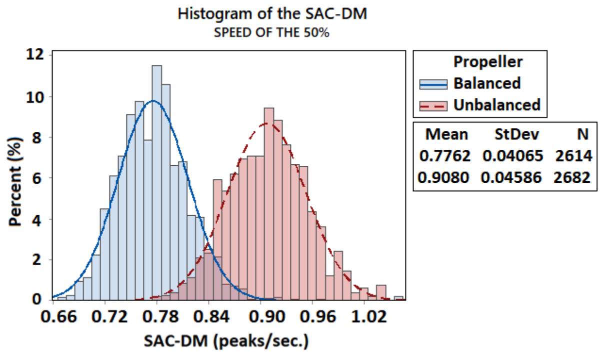


**FIGURE 12.** Histogram of the SAC-DM calculated from the sound signal with balanced and unbalanced propeller for 50% speed.

is 0.6%. This means the accuracy of 88.34% for detecting the motor speed when the propeller is unbalanced.

In Figure 12, the distribution of the SAC-DM values is shown for the motor with 50% of speed, now with balanced (blue) and unbalanced (red) propeller. The area of intersection between the presented histograms concerns the cases where the detection of unbalance would not be accurate. The remaining areas result in an unbalance detection accuracy of 92.63%.

The average values of all SAC-DM values for each motor speed (60%, 65%, 70%, 75%, and 80%) are shown in Figure 13, together with the tendency line for each of them. In this way, it is possible to estimate the approximate motor speed from the SAC-DM value.

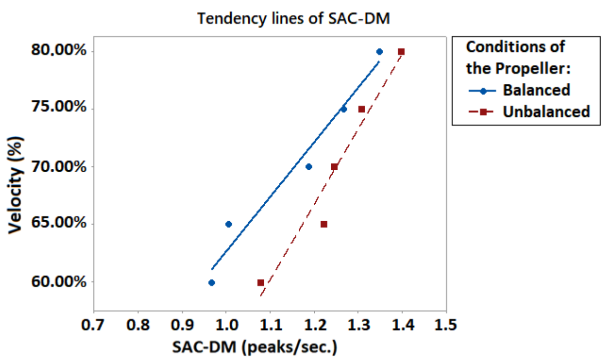


**FIGURE 13.** Average values and tendency lines for the SAC-DM, with balanced and unbalanced propeller.

Equation 9 and Equation 10 determine the relation between Speed(s) for balanced and unbalanced propeller, respectively, where $s$ is the value of SAC-DM:

$$\text{Speed}_{\text{balanced}}(s) = 0,47s + 0,15 \tag{9}$$

$$\text{Speed}_{\text{unbalanced}}(s) = 0,65s - 0,12 \tag{10}$$

## V. CONCLUSION

The similarity of the results between the values of the CLC and the SAC-DM in the scenarios tested here proves that the system has a chaotic behavior. However, SAC-DM uses a single and short time series to calculate the correlation coefficient. This technique uses the average density of maxima of sound samples to estimate the conditions of the BLDC motor.

Data analyzes using the SAC-DM, as well as the results obtained in the experiments, allow the detection of the unbalanced propeller in the motor running in a fixed and known speed. Besides, with SAC-DM, it is possible to estimate the speed at which the motor is operating. The experiments demonstrated that it was possible to detect the speed of the motor with an accuracy of 95.89% and to detect eccentricity problems when the motor is at 50% of speed with an accuracy of 88.34%. The method is entirely non-intrusive, which means that only a microphone and a micro-controller are necessary to implement a device to detect speed. A practical alternative for the diagnosis of unbalance problems is to keep the speed constant at a known value and run the SAC-DM.

The generalization of SAC-DM to analyze electric motors is under development and will be presented in future works. Here we focus on proving it is possible to detect eccentricity failure in BLDC motors using SAC-DM even with a single microphone. The plan is to apply this method in real-time analysis in small UAV, where BLDC motors are vastly used. Also, a set of sensors might be used to improve the variety of failures detected.

## REFERENCES

[1] J. Karthikeyan and R. D. Sekaran, "Current control of brushless DC motor based on a common DC signal for space operated vehicles," *Int. J. Elect. Power Energy Syst.*, vol. 33, no. 10, pp. 1721–1727, 2011. [Online]. Available: http://www.sciencedirect.com/science/article/pii/S0142061511001955

[2] Y. Zhao, H. Wang, D. Li, and R. Qian, "Fault-tolerant performance of a three-phase dual armature-winding doubly salient brushless DC generator," *IEEE Access*, vol. 6, pp. 18022–18031, 2018.

[3] L. Yang, J. Zhao, L. Yang, X. Liu, and L. Zhao, "Investigation of a statorironless brushless DC motor with non-ideal back-EMF," *IEEE Access*, vol. 7, pp. 28044–28054, 2019.

[4] K. Liu, Z. Zhou, and W. Hua, "A novel region-refinement pulse width modulation method for torque ripple reduction of brushless DC motors," *IEEE Access*, vol. 7, pp. 5333–5342, 2019.

[5] J. Kuzma, S. O'Sullivan, T. W. Philippe, J. W. Koehler, and R. S. Coronel, "Commercialization strategy in managing online presence in the unmanned aerial vehicle industry," *Int. J. Bus. Strategy*, vol. 17, no. 1, pp. 59–68, 2017. [Online]. Available: http://eprints.worc.ac.uk/5436/

[6] M. P. Mills. (2017). *Drone Disruption: The Stakes, the Players, and the Opportunities*. Accessed: Mar. 20, 2017. [Online]. Available: https://www.forbes.com

[7] C. Stöcker, R. Bennett, F. Nex, M. Gerke, and J. Zevenbergen, "Review of the current state of UAV regulations," *Remote Sens.*, vol. 9, no. 5, p. 459, 2017. [Online]. Available: http://www.mdpi.com/2072-4292/9/5/459/htm

[8] J. Straub and J. Huber, "Validating a UAV artificial intelligence control system using an autonomous test case generator," *Proc. SPIE*, vol. 8713, May 2013, Art. no. 87130I.

[9] E. Artigao, A. Honrubia-Escribano, and E. Gómez-Lázaro, "Current signature analysis to monitor DFIG wind turbine generators: A case study," *Renew. Energy*, vol. 116, pp. 5–14, Feb. 2018. [Online]. Available: http://www.sciencedirect.com/science/article/pii/S0960148117305165

[10] B. L. R. Samaga and K. P. Vittal, "Comprehensive study of mixed eccentricity fault diagnosis in induction motors using signature analysis," *Int. J. Elect. Power Energy Syst.*, vol. 35, no. 1, pp. 180–185, 2012. [Online]. Available: http://www.sciencedirect.com/science/article/pii/S0142061511002389

[11] A. Sapena-Bano, F. Chinesta, M. Pineda-Sanchez, J. V. Aguado, D. Borzacchiello, and R. Puche-Panadero, "Induction machine model with finite element accuracy for condition monitoring running in real time using hardware in the loop system," *Int. J. Elect. Power Energy Syst.*, vol. 111, pp. 315–324, Oct. 2019. [Online]. Available: http://www.sciencedirect.com/science/article/pii/S0142061518330126

[12] K. Kang, J. Song, C. Kang, S. Sung, and G. Jang, "Real-time detection of the dynamic eccentricity in permanent-magnet synchronous motors by monitoring speed and back EMF induced in an additional winding," *IEEE Trans. Ind. Electron.*, vol. 64, no. 9, pp. 7191–7200, Sep. 2017.

[13] S. Rajagopalan, J. M. Aller, J. A. Restrepo, T. G. Habetler, and R. G. Harley, "Analytic-wavelet-ridge-based detection of dynamic eccentricity in brushless direct current (BLDC) motors functioning under dynamic operating conditions," *IEEE Trans. Ind. Electron.*, vol. 54, no. 3, pp. 1410–1419, Jun. 2007.

[14] J.-K. Park and J. Hur, "Detection of inter-turn and dynamic eccentricity faults using stator current frequency pattern in IPM-type BLDC motors," *IEEE Trans. Ind. Electron.*, vol. 63, no. 3, pp. 1771–1780, Mar. 2016.

[15] C. Kral, T. G. Habetler, and R. G. Harley, "Detection of mechanical imbalances of induction machines without spectral analysis of time-domain signals," *IEEE Trans. Ind. Appl.*, vol. 40, no. 4, pp. 1101–1106, Jul. 2004.

[16] G. Georgoulas, V. Climente-Alarcon, J. A. Antonino-Daviu, I. P. Tsoumas, C. D. Stylios, A. Arkkio, and G. Nikolakopoulos, "The use of a multilabel classification framework for the detection of broken bars and mixed eccentricity faults based on the start-up transient," *IEEE Trans. Ind. Informat.*, vol. 13, no. 2, pp. 625–634, Apr. 2017.

[17] P. Konar and P. Chattopadhyay, "Multi-class fault diagnosis of induction motor using Hilbert and wavelet transform," *Appl. Soft Comput.*, vol. 30, pp. 341–352, May 2015. [Online]. Available: http://www.sciencedirect.com/science/article/pii/S1568494615000290

[18] I. Ouachtouk, S. El Hani, and K. Dahi, "Wireless health monitoring system for rotor eccentricity faults detection in induction machine," *Power Eng. Elect. Eng.*, vol. 15, pp. 376–384, Dec. 2017.

[19] A. Rezig, M. R. Mekideche, and A. Djerdir, "Effect of rotor eccentricity faults on noise generation in permanent magnet synchronous motors," *Progr. Electromagn. Res.*, vol. 15, pp. 117–132, Aug. 2010.

[20] E. T. Esfahani, S. Wang, and V. Sundararajan, "Multisensor wireless system for eccentricity and bearing fault detection in induction motors," *IEEE/ASME Trans. Mechatronics*, vol. 19, no. 3, pp. 818–826, Jun. 2014.

[21] D. Bazeia, M. B. P. N. Pereira, A. V. Brito, B. de Oliveira, and J. G. G. S. Ramos, "A novel procedure for the identification of chaos in complex biological systems," *Sci. Rep.*, vol. 7, Mar. 2017, Art. no. 44900.

[22] R. L. V. Medeiros, J. G. G. S. Ramos, T. P. Nascimento, A. C. L. Filho, and A. V. Brito, "A novel approach for brushless DC motors characterization in drones based on chaos," *Drones*, vol. 2, no. 2, p. 14, 2018. [Online]. Available: http://www.mdpi.com/2504-446X/2/2/14

[23] R. L. V. Medeiros, A. C. L. Filho, J. G. G. S. Ramos, T. P. Nascimento, and A. V. Brito, "A novel approach for speed and failure detection in brushless DC motors based on chaos," *IEEE Trans. Ind. Electron.*, vol. 66, no. 11, pp. 8751–8759, Nov. 2019.

[24] A. Glowacz, W. Glowacz, Z. Glowacz, and J. Kozik, "Early fault diagnosis of bearing and stator faults of the single-phase induction motor using acoustic signals," *Measurement*, vol. 113, pp. 1–9, Jan. 2018.

[25] A. Glowacz and Z. Glowacz, "Diagnosis of stator faults of the single-phase induction motor using acoustic signals," *Appl. Acoust.*, vol. 117, pp. 20–27, Feb. 2017. [Online]. Available: http://www.sciencedirect.com/science/article/pii/S0003682X16303401

[26] A. Glowacz, "Fault diagnosis of single-phase induction motor based on acoustic signals," *Mech. Syst. Signal Process.*, vol. 117, pp. 65–80, Feb. 2019. [Online]. Available: http://www.sciencedirect.com/science/article/pii/S0888327018304448

[27] A. Glowacz, "Acoustic based fault diagnosis of three-phase induction motor," *Appl. Acoust.*, vol. 137, pp. 82–89, Aug. 2018. [Online]. Available: http://www.sciencedirect.com/science/article/pii/S0003682X18300951

[28] M. A. Nowak and R. M. May, "Evolutionary games and spatial chaos," *Nature*, vol. 359, no. 6398, pp. 826–829, 1992.

[29] M. Mitchell, J. P. Crutchfield, and P. T. Hraber, "Revisiting the edge of chaos: Evolving cellular automata to perform computations," *Complex Syst.*, vol. 7, pp. 89–130, 1993.

[30] G. Károlyi, Z. Neufeld, and I. Scheuring, "Rock-scissors-paper game in a chaotic flow: The effect of dispersion on the cyclic competition of microorganisms," *J. Theor. Biol.*, vol. 236, no. 1, pp. 12–20, 2005.

[31] M. Gosak, M. Marhl, and M. Perc, "Chaos between stochasticity and periodicity in the Prisoner's dilemma game," *Int. J. Bifurcation Chaos*, vol. 18, no. 3, pp. 869–875, 2008.

[32] R. W. Hamming, "Error detecting and error correcting codes," *Bell Syst. Tech. J.*, vol. 29, no. 2, pp. 147–160, Apr. 1950.

[33] J. G. G. S. Ramos, D. Bazeia, M. S. Hussein, and C. H. Lewenkopf, "Conductance peaks in open quantum dots," *Phys. Rev. Lett.*, vol. 107, no. 17, 2011, Art. no. 176807.

[34] A. G. A. Cruz, R. D. Gomes, F. A. Belo, and A. C. L. Filho, "A hybrid system based on fuzzy logic to failure diagnosis in induction motors," *IEEE Latin Amer. Trans.*, vol. 15, no. 8, pp. 1480–1489, Jul. 2017.

[35] S. Mallat, *A Wavelet Tour of Signal Processing: The Sparse Way*, 3rd ed. New York, NY, USA: Academic, 2008.


**FRANK CESAR VERAS** graduated in technologist in data processing from the Association of Higher Education of Piau, in 2000. He received the master's degree in informatics from the Federal University of Paraiba—UFPB, whose thesis: Modeling and Simulation of Displacement of People to Estimate Group Formation, was defended in Feb 2013, and the master's degree in computer science in education from the Universidade Federal de Lavras—MG, in 2004. He has been an Assistant Professor of the Information Systems Course of the Federal University of Piau—Campus Senator Helvdio Nunes de Barros, since 2006. He is currently pursuing the Ph.D. degree in Eng. Mecinica with the Federal University of Paraiba (UFPB), with emphasis on dynamics and systems control, whose qualification was entitled A chaos-based approach to speed detection and DC motor anomaly without brushing from beeps.

**THYAGO L. V. LIMA** received the degree in industrial automation from the Federal Institute of Education, Science, and Technology of Paraiba and the master's degree in mechanical engineering from the Federal University of Paraiba, in 2012. He is currently a Professor of basic education, technical, and technological with the Federal Institute of Education, Science, and Technology of Paraiba.

**JEFFERSON S. SOUZA** received a technical course and the degree in technology in systems for internet from the Federal Institute of Education, Science, and Technology of Paraiba, in 2004. He is currently pursuing the master's degree in computer science with the Federal University of Paraiba. He is a Software Engineer with Phoebus Tecnologia.

**JORGE G. G. S. RAMOS** received the bachelor's degree in physics from the Federal University of Paraiba, UFPB, in 2003, the Ph.D. degree in physics from the Federal University of Pernambuco, UFPE, in 2010, and the postdoc in physics from the University of So Paulo, USP, in 2011. He has experience in the area of physics, with emphasis on electronic transportation and electrical properties of surfaces, interfaces, and films, working mainly in the following subjects: quantum transport, quantum chaos, and mesoscopic systems. He is currently an Associate Professor with the Federal University of Paraiba, Brazil.

**ABEL C. LIMA FILHO** was born in Maceio, Brazil, in 1980. He received the B.S. degree in electrical engineering from the Federal University of Campina Grande, Campina Grande, Brazil, in 2004, and the M.S. and D.S. degrees in mechanical engineering from the Federal University of Paraiba, Joao Pessoa, Brazil. Since 2010, he has been with the Mechanical Engineering Department, Federal University of Paraiba, where he is currently a Professor. His research interests include telemetry, embedded systems, fault diagnostics, and instrumentation.

**ALISSON V. BRITO** received the BA and master's degrees in computer science and the Ph.D. degree in electrical engineering from the Federal University of Campina Grande (UFCG), Brazil, in microelectronics, in 2001, 2003, and 2008, respectively, with cooperation with the Karlsruhe Institute of Technology (KIT), Germany. He has experience in computer science, with emphasis on design and development of embedded systems, mainly in the following themes: design and simulation of embedded systems and applications using unmanned aerial vehicles. Since 2019, he has been an Associate Professor with the Federal University of Paraiba (UFPB). He is a Coordinator of the Laboratory of System Engineering and Robotics (LASER) and works on the Graduate Program in Computer Science (PPGI) at UFPB, where he teaches courses mainly in the areas of computer architecture and embedded systems.